THE BIVARIATE BRIGHTNESS DISTRIBUTIONS OF BULGES AND DISKS

J. Liske[1], S.P. Driver[2] and P.D. Allen[2]

[1] *ESO, Karl-Schwarzschild-Str. 2, 85748 Garching bei München, Germany*
[2] *RSAA, Mount Stromlo Observatory, Cotter Road, Weston Creek ACT 2611, Australia*

Abstract.
   Galaxy bulges and disks are thought to form and evolve by two distinct mechanisms: mergers and accretion. Testing this fundamental feature of galaxy formation models requires the bulge-disk decomposition of large, well-defined samples. Here we report results from the bulge-disk decomposition of 10 000 galaxies drawn from the Millennium Galaxy Catalogue (MGC). The MGC is a local survey (median $z = 0.12$) spanning 31 deg^2, and it combines the size, depth (26 mag arcsec^{-2}) and high redshift completeness (96%) that are necessary to avoid serious selection biases. We present the joint luminosity and surface brightness distributions of bulges and disks. The aim is to provide a $z = 0$ data point for comparison with higher redshift observations and theory.

1   Introduction

The bivariate brightness distribution (BBD) quantifies the space density of galaxies as a joint function of luminosity and surface brightness and is hence an extension of the luminosity function. The BBD is linked to the mass and angular momentum distributions of galaxies and the different formation processes of different galaxy types or components are thought to be encoded in their BBDs, e.g. [1], [2], [3]. The evolution of the mass and angular momentum distributions can be predicted from simulations with some confidence, e.g. [4], and hence the BBD is a useful testbed for galaxy formation models. Constructing the BBDs of disks and bulges separately is of particular interest in this respect. However, at $z = 0$ this requires high-quality, wide-field imaging data with well known selection limits, and a corresponding redshift survey to high completeness.

   In [5] we recently presented the BBD of local galaxies using their *global* or *total* luminosities and surface brightnesses. In this contribution we present our first (and preliminary) results on the separate bulge and disk BBDs, i.e. using the *component* luminosities and surface brightnesses.

2   Data: The Millennium Galaxy Catalogue

The Millennium Galaxy Catalogue (MGC; [6], [5]) is a deep, wide-field B-band imaging survey conducted with the Wide Field Camera on the INT, covering 31 deg^2 in ~ 1.25 arcsec seeing to a limiting isophote of 26 mag arcsec^{-2}. Details of the observations, data reduction, object detection and catalogue construction are given in [6]. The galaxy sample used here is defined as the 10 095 MGC galaxies that have $13 < B < 20$ mag.

   To obtain redshifts for this sample we have performed a redshift survey using 2dF, which complements publicly available data from the SDSS and 2dFGRS. However, using a fibre-fed MOS like 2dF inevitably introduces a surface brightness bias in the redshift completeness. To mitigate this effect we have supplemented our redshift survey with a single-slit campaign on Gemini, the NTT, the TNG and the ANU 2.3m. The final redshift completeness is 96.05% and we show the distribution of the incompleteness as a function of magnitude and surface brightness in Fig. 1. The median redshift of our sample is 0.12. More details on the redshift survey are given in [5].

   The excellent MGC image quality enables us to decompose all galaxies with $B < 20$ mag into bulges and disks using GIM2D [7]. The MGC is currently one of the largest samples for which quantitative morphology is available. The 2D surface brightness profile is modelled as the sum of a Sérsic bulge and an exponential disk, convolved with the seeing (see P. Allen's contribution to these proceedings for details). We have confirmed the reliability of this process using independent duplicate observations of ~ 700 objects in the overlap regions of neighbouring MGC fields.

   In Fig. 2 we show the distributions of the extracted disks and bulges in various component parameter spaces. It appears that the bulges (shown in red and green) may in fact consist of two populations (hence the different colours). For example, in the left panel of Fig. 2 the bulges form a distinct cloud in the upper right of the plot but there is also a scattering of points towards the lower left. Here we have chosen to separate the two populations by a simple cut in the colour-central surface brightness plane, shown as a solid line in the middle panel of Fig. 2. Following visual inspection of the MGC images of a subset of these objects we tentatively interpret the redder, higher surface brightness, higher Sérsic index population as the 'real' bulges and spheroids. The other
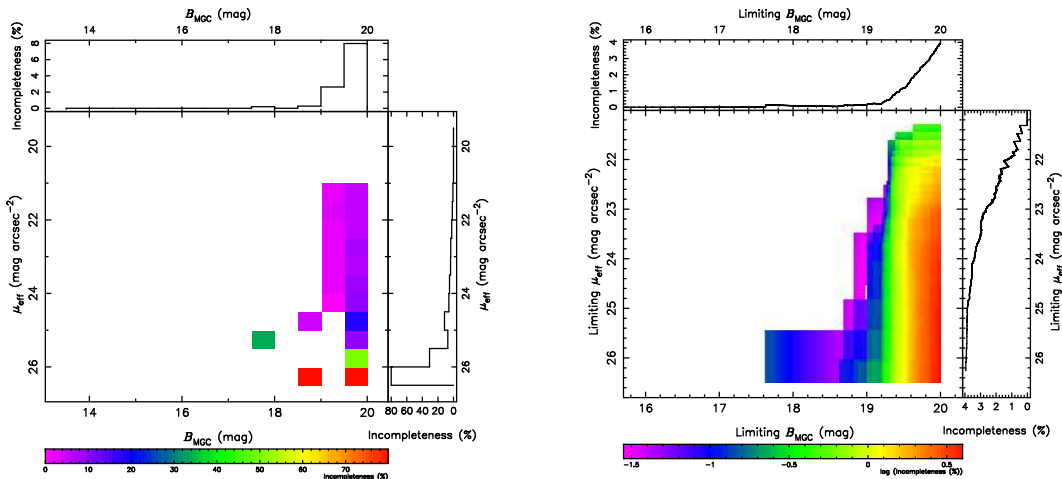
Figure 1: The MGC's overall redshift incompleteness is 96.05%. The left panel shows the incompleteness as a function of magnitude and surface brightness. Despite our single-slit observations some magnitude and surface-brightness-dependent bias still remains. We account for this in the analysis. The right panel shows the incompleteness as a function of *limiting* magnitude and surface brightness. From the top sub-panel we can see that for $B < 19.2$ mag the incompleteness is only 0.21%.

population seems to be less homogeneous, containing bars, cores, inner disks and probably pseudobulges [8]. In the following we will treat these classes separately and refer to them as real and pseudo bulges.

3 Constructing BBDs

To construct the separate BBDs we use the component magnitudes and half-light-radii returned by GIM2D and the 2D step-wise maximum likelihood method described in detail in [5]. In summary, the procedure consists of the following steps:

1. Determine the selection limits on the observables and reject all objects beyond these limits where the survey must be deemed incomplete. Apart from the imposed magnitude limits, the selection limits consist of the maximum and minimum size and a limiting effective surface brightness. Understanding these limits in detail is non-trivial. For example, the detectability of a given disk does not only depend on the disk's magnitude, size and surface brightness but also on the parameters of its bulge (if it has one). A proper analysis of these effects is still pending. Here we conservatively set the low-surface brightness and maximum size limits to the same values as in [5]'s analysis of the total-galaxy BBD, i.e. $\mu_{lim} = 25.25$ mag arcsec^{-2} and $r_{max} = 15$ arcsec. These are not absolute detection limits but rather the limits to which accurate photometry is possible. The minimum size limit is determined by GIM2D's capability of recovering a component half-light radius, and we set it to 0.7 times the FWHM of the seeing. These cautious limits leave us with complete samples of 5721 disks, 1160 real bulges and 559 pseudo bulges.

2. Attach a weight to each object according to the redshift incompleteness in its observed magnitude-surface brightness bin (cf. Fig. 1).

3. Reject objects outside of the redshift limits: $0.013 < z < 0.18$. Peculiar velocities dominate below the lower limit, while the upper limit is the redshift at which M^* objects fall below our faint magnitude limit.

4. Calculate luminosities and effective surface brightnesses using the evolutionary and k-corrections of [5], $H_0 = 100\ h$ km/s/Mpc, $\Omega_M = 0.3$ and $\Omega_\Lambda = 0.7$.

5. Apply SWML iteration, making use of the selection limits determined in step 1. above and the incompleteness weights from step 2.

6. Normalise. Here we use the simplest possible normalisation scheme by requiring the final BBD to reproduce the (incompleteness corrected) observed number of objects in a representative part of the (M_B, μ, z) parameter space.
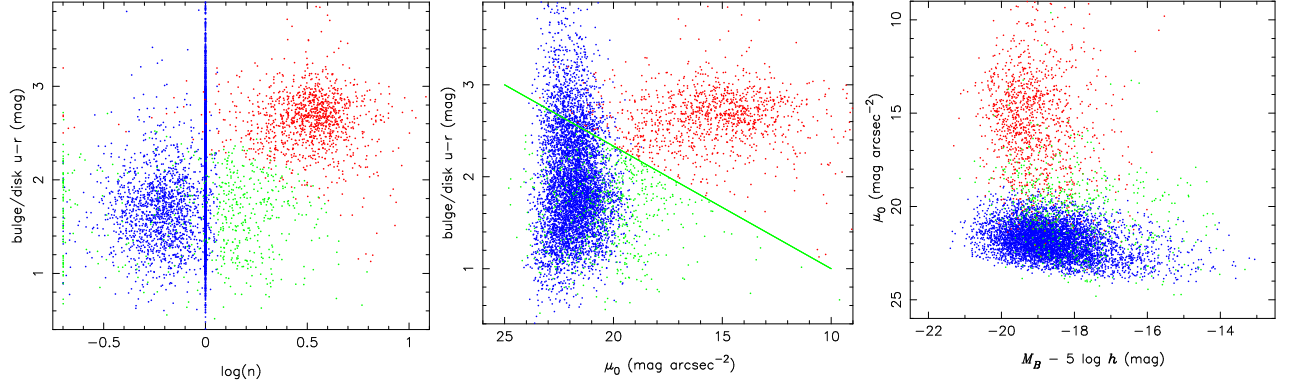
Figure 2: The distributions of MGC bulges and disks in various component parameter spaces: $u - r$ colour (from SDSS photometry), Sérsic index (n), central surface brightness (μ_0), and luminosity (M_B). Disks are shown in blue, real bulges in red and pseudo bulges in green (see text). We separate the latter two classes by the solid line in the middle panel.
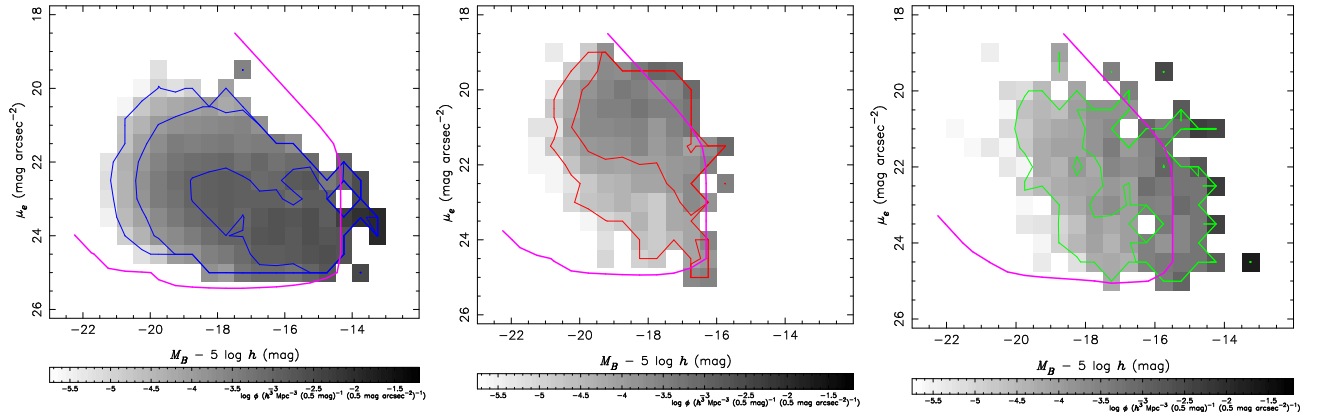

Figure 3: Preliminary BBDs of disks (left), real bulges (middle) and pseudo bulges (right). Both the contours and the grey-scale images show the space density ϕ in logarithmic units. The thick solid line in each panel shows the selection limit, arbitrarily defined as the boundary of the region where at least 100 objects could have been detected.
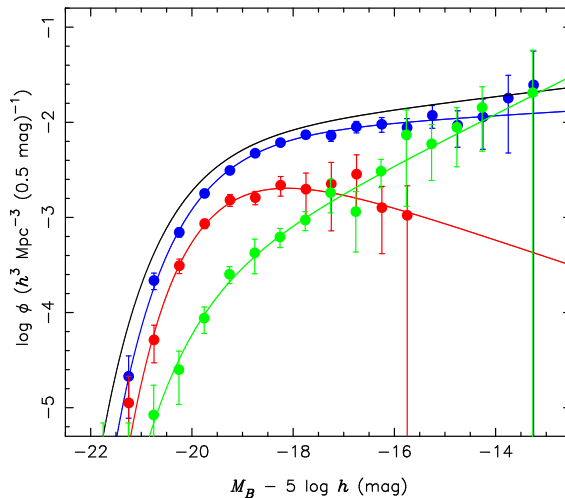
Figure 4: Luminosity functions of disks (blue, second from top at the bright end), real bulges (red, third from top) and pseudo bulges (green, lowest at the bright end) obtained by integrating the respective BBDs over surface brightness. For comparison, the black (top) line shows the global MGC luminosity function.

4 Results

Fig. 3 shows the component BBDs resulting from the above process. The disk BBD exhibits a well-defined shape: at a given luminosity the distribution of surface brightness is Gaussian, i.e. the size distribution of disks is log-normal. The peak of the surface brightness distribution shifts to fainter values at lower luminosities. This surface brightness-luminosity relation is described by $\mu^* = 21.78 + 0.5\,(M_B + 20)$ mag arcsec^{-2}, which is not too dissimilar to the relation found by [3]. At $M_B > -16$ mag the distribution runs into the selection boundary and even the MGC is not deep enough to probe the faint, low-surface brightness dwarf disks. However, at brighter magnitudes the distribution falls off to zero *before* reaching the selection boundary and hence there is no evidence of a substantial giant low-surface brightness disk population.

The real and pseudo bulge BBDs are much less well defined than the disk BBD, due to the smaller number of objects. The pseudo bulge BBD in particular does not currently provide any useful results. However, the contours of the real bulge BBD shows a hint of a luminosity-surface brightness relation which goes in the opposite sense to that of the disks: lower luminosity systems have higher surface brightnesses. This is reminiscent of the Kormendy relation, however in detail the relation does not seem to fit our data because it has a steeper slope and is shifted towards higher surface brightnesses.

Finally, in Fig. 4 we present the component luminosity functions obtained by integrating the BBDs of Fig. 3 over surface brightness.

5 Summary

We have performed bulge-disk decomposition of $\sim 10\,000$ local galaxies with $B < 20$ mag drawn from the Millennium Galaxy Catalogue. We found evidence that the bulges are 'contaminated' by a variety of structures frequently found in the central regions of galaxies, such as bars, inner disks, pseudobulges, etc. Having crudely separated these systems from the 'real' bulges we have constructed preliminary versions of the bivariate brightness distributions of disks and bulges, i.e. their space densities as a joint function of luminosity and surface brightness. We found that disks and bulges behave quite differently in this plane, qualitatively recovering known trends derived from small, ad hoc selected samples. However, more work is required before meaningful detailed comparisons with these trends, other data or models can be performed.

References

[1] Dalcanton J.J., Spergel D.N., Summers F.J., ApJ, 482, 659, 1997

[2] Mo H.J., Mao S., White S.D.M., MNRAS, 295, 319, 1998

[3] de Jong R.S., Lacey C., ApJ, 545, 781, 2000

[4] Bullock J.S., Dekel A., Kolatt T.S., Kravtsov A.V., Klypin A.A., Porciani C., Primack J.R., ApJ, 555, 240, 2001

[5] Driver S.P., Liske J., Cross N.J.G., De Propris R., Allen P.D., MNRAS, 360, 81, 2005

[6] Liske J., Lemon D.J., Driver S.P., Cross N.J.G., Couch W.J., MNRAS, 344, 307, 2003

[7] Simard L., 1998, in ASP Conf. Ser. 145: Astronomical Data Analysis Software and Systems VII, 145, 108

[8] Kormendy R.C., Kennicutt J., ARA&A, 42, 603, 2004